

CALCULATION OF SCATTERING BY THE DISTORTED WAVE BORN APPROXIMATION

Kathie E. Newman and Eytan Domany
Department of Physics, University of Washington
Seattle, Wa 98195

ABSTRACT

An approximate scattering theory that utilizes the exact solutions for spherical defects is being developed. A defect of arbitrary shape can be represented by a sphere S and a remainder volume δv . By treating δv as a perturbation, one obtains an approximate solution that contains non-trivial frequency dependence and phase information. The approach is expected to be useful for studying defects with small but significant deviations (such as sharp edges) from spherical shape.

INTRODUCTION

The basic problem of defect characterization by ultrasonic techniques has received considerable attention in recent years. Two different but complementary aspects of the problem have been approached. These are known as the direct and inverse problems. The direct problem is that of calculating the scattering of elastic waves from a known defect. The inverse problem is that of characterizing an unknown defect from a set of measured scattered waves. Obviously, these two are closely related. Solutions of either provide clues as to what measurements to perform and which features of the scattered power would be the most useful for defect characterization.

Due to the considerable mathematical complexity inherent in solving for elastic wave scattering, exact solutions are available for only a small number of scatterer geometries. This has led to the development of approximate solutions such as the Born Approximation¹ (BA) and the Quasi Static Approximation² (QSA). The BA is useful for obtaining information on the angular distribution of frequency averaged power.³ However, it is known³ to yield quite unreliable frequency dependence for the scattered power. The QSA is exact in the long wavelength limit; recently suggested inversion procedures based on the frequency dependence (extrapolated to low frequencies) show great promise^{4,5}. The QSA is unfortunately limited to ellipsoidal scatterers, for which exact solutions based on T-matrix expansion methods also exist⁶. Neither the BA nor the QSA are capable of calculating phase information.

In the investigation reported here we aim at filling various gaps in the existing approximate solutions. We hope to obtain an approximation scheme that will provide non trivial phase information and more reliable frequency dependence over a wider range of frequencies. At the same time we aim at obtaining information about non elliptical defects.

The motivation is quite obvious. Past experience indicates that the frequency dependence is very useful in defect characterization^{3,7,8}. Frequency dependence is also a much more flexible experimental tool than the study of angular distribution, since a wide range of frequencies can be

studied in a single (broad band) experiment. We believe that an efficient inversion procedure will have to build from reliable frequency information. Reliable frequency dependence of phase information⁸ should be also incorporated into an inversion procedure. Finally, since present models of inversion rely on representing a general defect by an effective ellipsoid, we feel that a generalization of the direct problem to non-ellipsoidal shapes is important. We hope to investigate the effects of sharp edges and surface roughness, topics that may be most relevant in the NDE context.

THE DISTORTED WAVE BORN APPROXIMATION

The DWBA is based on a perturbative solution of the scattering equation, much in the same way as the Born Approximation. However, while in the BA the unperturbed problem (or zeroth order solution) is the incident wave¹ (propagating in a homogeneous medium with no defect), the DWBA uses the solutions of the scattering problem for a spherical defect¹⁰ as the unperturbed zeroth order approximation. Thus, while the BA is exact only in the limit of vanishing difference between the properties of medium and defect, the DWBA has an additional "small parameter", i.e. a measure of the deviation of the defect from spherical. As shown below, in order to calculate the scattered wave within the DWBA, one needs the Green's function, g^S , of an infinite medium with a spherical defect. When g^S is approximated by the infinite medium Green's function g^0 , we obtain an approximation expected to be of intermediate quality between BA and DWBA. In this paper we present results based on the intermediate approximation. Work aimed at evaluating g^S is in progress; when g^S is obtained, we hope to use it in the existing integration routines, thus obtaining the DWBA.

To present a precise statement of the ideas discussed above, consider the differential equation for the propagation of elastic waves in a medium, characterized by the (position dependent) elastic constants C_{ijkl} and density ρ , given by

$$C_{ijkl}u_{k,jl} + \rho\omega^2 u_i = 0 \quad (1)$$

where u_i is the displacement field and ω the frequency. Consider the geometry depicted in Fig. 1, i.e.,

$$c(\underline{r}) = c^0 + \theta_R(\underline{r}) \delta c,$$

$$\rho(\underline{r}) = \rho^0 + \theta_R(\underline{r}) \delta \rho \quad (2)$$

where $\theta(r) = 1$ if $\underline{r} \in R$, and zero otherwise. The defect R is separated into two regions: a spherical one (S) and a remainder \bar{R} , such that $R = S + \bar{R}$. Then one can define $\theta_S(\underline{r})$ and $\theta_{\bar{R}}(\underline{r})$ in a similar way, so that (see Fig. 1)

$$\theta_R(\underline{r}) = \theta_S(\underline{r}) + \theta_{\bar{R}}(\underline{r}). \quad (3)$$

$$R = S + \bar{R}$$

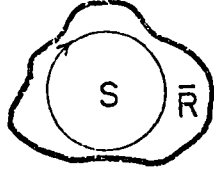


Fig. 1 The defect R is represented as a sphere S and a "remainder" volume \bar{R} .

We can now consider as our unperturbed problem the case where only the spherical defect S is present. To do this, define

$$\begin{aligned} c^S(\underline{r}) &= c^0 + \theta_S(\underline{r}) \delta c \\ \rho^S(\underline{r}) &= \rho^0 + \theta_S(\underline{r}) \delta \rho, \end{aligned} \quad (4)$$

and we can obviously write

$$\begin{aligned} c(\underline{r}) &= c^S(\underline{r}) + \theta_{\bar{R}}(\underline{r}) \delta c \\ \rho(\underline{r}) &= \rho^S(\underline{r}) + \theta_{\bar{R}}(\underline{r}) \delta \rho. \end{aligned} \quad (5)$$

Using now (5) in (1), the scattering equation takes the form

$$c_{ijkl}^S u_{k,jl} + \rho \omega^2 u_i = -\theta_{\bar{R}} \left[\delta c_{ijkl} u_{k,jl} + \omega^2 \delta \rho u_i \right] \quad (6)$$

If the right hand side vanishes, the solutions of this equation are the scattered waves by a spherical defect, obtained previously by various investigators. These solutions have been programmed and are readily evaluated numerically. Proceeding in a similar fashion as Gubernatis et al., we obtain the integral equation

$$\begin{aligned} u_i(\underline{r}) &= u_i^S(\underline{r}) + \delta \rho \omega^2 \int_{\bar{R}} d\underline{r}' g_{im}^S(\underline{r}, \underline{r}') u_m(\underline{r}') \\ &\quad - \delta c_{jklm} \int_{\bar{R}} d\underline{r}' g_{ij,k}^S(\underline{r}, \underline{r}') u_{l,m}(\underline{r}'), \end{aligned} \quad (7)$$

where $u_i^S(\underline{r})$ is the solution of the scattering problem with a spherical defect only, i.e.,

$$c_{ijkl}^S u_{k,jl} + \rho^S \omega^2 u_i = 0, \quad (8)$$

and $g_{im}^S(\underline{r}, \underline{r}')$ is the Green's function in the presence of a spherical defect, i.e.,

$$c_{ijkl}^S g_{km,jl}^S(\underline{r}, \underline{r}') + \rho^S \omega^2 g_{im}^S(\underline{r}, \underline{r}') = -\delta_{im} \delta(\underline{r} - \underline{r}'). \quad (9)$$

Note that in equation (7)

$$g_{im,j}^S(\underline{r}, \underline{r}') = \frac{\partial}{\partial r_j} g_{im}^S(\underline{r}, \underline{r}') \quad (10)$$

and that since c_{ijkl}^S and ρ^S are not translationally invariant, $g_{ij}^S(\underline{r}, \underline{r}')$ is not a function of $\underline{r} - \underline{r}'$ only. The i,j -DWBA consists of replacing $u_i(\underline{r}')$ in the integrands on the right hand side of equation (7) by $u_i^S(\underline{r}')$:

$$\begin{aligned} u_i^{DWB}(\underline{r}) &= u_i^S(\underline{r}) + \delta \rho \omega^2 \int_{\bar{R}} d\underline{r}' g_{im}^S(\underline{r}, \underline{r}') u_i^S(\underline{r}') \\ &\quad - \delta c_{jklm} \int_{\bar{R}} d\underline{r}' g_{ij,k}^S(\underline{r}, \underline{r}') u_{l,m}^S(\underline{r}') \end{aligned} \quad (11)$$

To evaluate u_i^{DWB} , we need the functions u_i^S and g_{ij}^S , and perform the integration over the region \bar{R} numerically. The relative corrections to the Born approximation are of order $R\delta C$; to the DWBA of order $\delta C R/S$. This means that we introduced a geometrical "small parameter", namely the deviation of the defect from spherical. We also hope to determine the "optimal sphere" to be used for treatment of various defects. Since the function g^S has not been calculated previously, we start by setting up an intermediate approximation, replacing g^S in equation (11) by the infinite medium Green's function g^0 . Since g^S satisfies an equation of the form (schematic)

$$g^S = g^0 + \int_S \delta C g^0 g^S$$

the error caused by replacing g^S by g^0 in (11) is of order $R\delta C \cdot S\delta C$. This intermediate approximation is given by

$$\begin{aligned} u_i^I &= u_i^S + \delta \rho \omega^2 \int_{\bar{R}} d\underline{r}' g_{im}^0(\underline{r} - \underline{r}') u_i^S(\underline{r}') \\ &\quad + \delta c_{jklm} \int_{\bar{R}} d\underline{r}' g_{ij,k}^0(\underline{r} - \underline{r}') u_{l,m}^S(\underline{r}') \end{aligned} \quad (12)$$

(where we used $g_{im,j}^0 = -g_{im,j}^0$).

To calculate the scattered power and phase, the observation point \underline{r} is taken to infinity.

Asymptotic forms for $u_i^S(\underline{r})$ are found for the spherical solution $u_i^S(\underline{r})$ (outside the integral only) and, in a manner similar to Gubernatis et al.⁹ for the Green's function. In the limit $r \rightarrow \infty$, the scattered wave can be written

$$u_i^{\text{scatt}} \sim \frac{e^{i\alpha r}}{r} A_i + \frac{e^{i\beta r}}{r} B_i \quad (13)$$

where α, β are the longitudinal and shear wave numbers respectively. A_i and B_i can be broken into a piece from the integral and a piece from the spherical solution,

$$\begin{aligned} A_i &= A_i^S + A_i^{\text{int}} \\ B_i &= B_i^S + B_i^{\text{int}} \end{aligned} \quad (14)$$

where A_i^{int} and B_i^{int} are given in general by

$$\begin{aligned} A_i^{\text{int}} &= \hat{r}_i \hat{r}_j f_j(\alpha) \\ B_i^{\text{int}} &= (\delta_{ij} - \hat{r}_i \hat{r}_j) f_j(\beta) \end{aligned} \quad (15)$$

and

$$\begin{aligned} f_i(\underline{k}) &= \frac{k^2}{4\pi\rho\omega^2} \left(\delta\rho\omega^2 \int_{\mathbb{R}} dV' u_i^S(\underline{r}') \exp(-i\underline{k} \cdot \underline{r}') \right. \\ &\quad \left. + i k \hat{r}_j \delta C_{ijkl} \int_{\mathbb{R}} dV' u_{k,l}(\underline{r}') \exp(-i\underline{k} \cdot \underline{r}') \right). \end{aligned} \quad (16)$$

For an incident longitudinal plane wave $\hat{z} e^{i\alpha z}$, A_i^S and B_i^S are calculated from the solution to the spherical problem¹⁰

$$\begin{aligned} A_i^S &= -i\alpha \sum_m (2m+1) A_m^* P_m(\cos\theta) \\ B_i^S &= i\alpha \sum_m (2m+1) B_m^* \frac{dP_m(\cos\theta)}{d\theta} \end{aligned} \quad (17)$$

where A_m, B_m are defined by Johnson-Trueell¹⁰

The longitudinal and shear differential cross sections are defined in the same way as Gubernatis et al.⁹

$$\begin{aligned} \frac{dP_\ell(\omega)}{d\Omega} &= |A_\ell|^2, \\ \frac{dP_t(\omega)}{d\Omega} &= |B_\ell|^2. \end{aligned} \quad (18)$$

The phase angles δ_ℓ and δ_t are defined from

$$\tan \delta_\ell = \frac{\text{Im} A_\ell}{\text{Re} A_\ell},$$

$$\tan \delta_t = \frac{\text{Im} B_\ell}{\text{Re} B_\ell}. \quad (19)$$

The results summarized in the following section are based on equations (18) and (19).

RESULTS

Prior to using the method we performed various checks. First we checked the accuracy of our numerical integration procedure.¹¹ To do this, we made use of the integral equation for an elastic wave u_i^0 scattered off a sphere of radius a ;

$$\begin{aligned} u_i(\underline{r}) &= u_i^0(\underline{r}) - \delta\rho\omega^2 \int_S dV' g_{im}^0(\underline{r}, \underline{r}') u_m^q(\underline{r}') \\ &\quad - \delta C_{jklm} \int_S dV' g_{ij,k}^0(\underline{r}, \underline{r}') u_{l,m}^q(\underline{r}') \end{aligned} \quad (20)$$

We employ the notation of Johnson and Trueell, where the total displacement wave solution is given by

$$u_i(\underline{r}) = \begin{cases} u_i^q(\underline{r}) & r < a \\ u_i^0(\underline{r}) + u_i^S(\underline{r}) & r > a \end{cases} \quad (21)$$

In the limit $r \rightarrow \infty$, the asymptotic form of the integral is given by

$$- \left(A_i^{\text{int}} \frac{e^{i\alpha r}}{r} + B_i^{\text{int}} \frac{e^{i\beta r}}{r} \right). \quad (22)$$

and the asymptotic form of $u_i^S(\underline{r})$ for incident longitudinal plane wave by

$$A_i^S \frac{e^{i\alpha r}}{r} + B_i^S \frac{e^{i\beta r}}{r} \quad (23)$$

We thus can numerically compare A_i^S and $-A_i^{\text{int}}$ and B_i^S and $-B_i^{\text{int}}$. Note that this comparison checks both numerical integration and the calculation of the expansion coefficients for the spherical function because the A_i^S, B_i^S use the expansion outside the sphere and the $A_i^{\text{int}}, B_i^{\text{int}}$ use the inside expansion. We were able to reduce our numerical error to $\sim 1\%$ by choice of a sufficiently fine grid.

As a check on the approximation method itself we evaluated the scattering by a large spherical defect, using a small sphere as the unperturbed problem. We considered two cases with incident longitudinal wave for both.

1. Al Flaw in Ti, with a ratio of 2 between the radii of the two spheres. For example, this amounts to calculating the scattering by a spherical defect of radius 400μ , using the solution of

the scattering by a defect of 200μ as our zeroth order approximation, and treating the volume difference between the two spheres as a perturbation. Note that the volume of the perturbation defect is seven times the unperturbed defect volume!

Thus the results presented below serve as a quite strong test on treatment of large volume deviations by our technique. The results for scattered power and phase as functions of ka , for the backscattered longitudinal wave are presented in Fig. 2, and for the mode converted shear wave (at 90°) on Fig. 3.

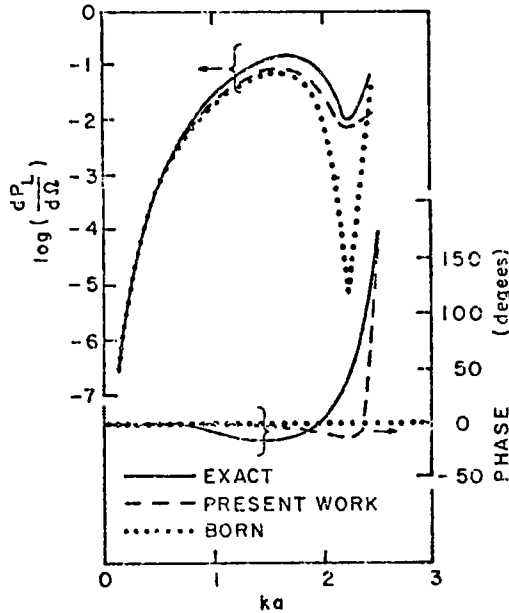


Fig. 2 Al sphere in Ti: Longitudinal backscattered wave, power and phase versus ka for a ratio of radii of 2.

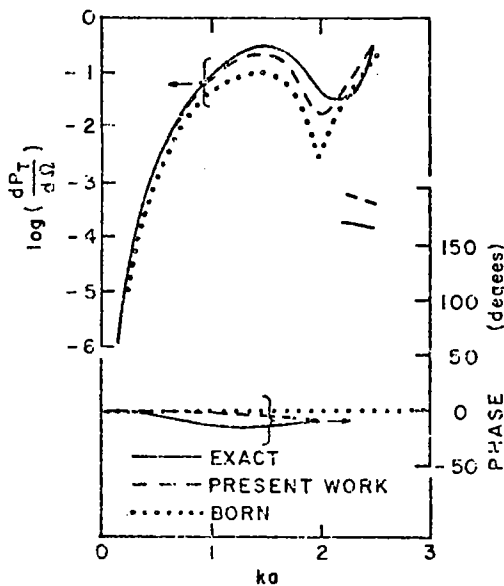


Fig. 3 Al sphere in Ti: Mode converted shear wave scattered at $\theta = 90^\circ$, power and phase versus ka for a ratio of radii of 2.

2. Spherical Cavity in Ti - Since the cavity constituted a much stronger defect than an aluminum inclusion, we chose to investigate a situation where radii of the actual defect and the one used as zeroth order approximation are closer, namely a ratio of $4/3$. Still, this corresponds (see Fig. 1) to $\bar{R}/S = 1.37$, i.e. we still deal with a rather large perturbation. The results for backscattered longitudinal and the mode converted shear wave at 90° are shown in Figs. 4 and 5, as plotted versus ka , and on Fig. 6 and 7, for $ka = 2$, plotted vs the scattering angle.

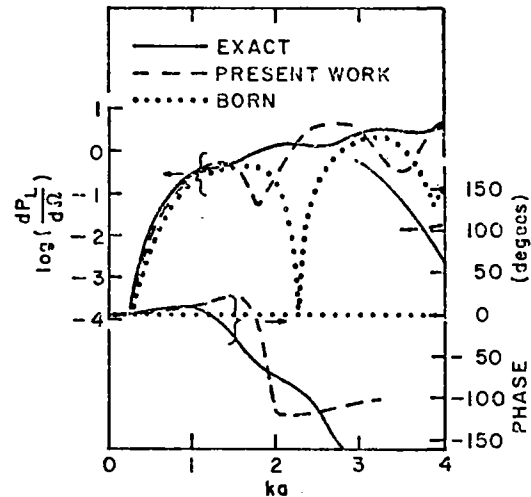


Fig. 4 Spherical cavity in Ti: Longitudinal backscattered wave, power and phase versus ka for a ratio of radii of $4/3$.

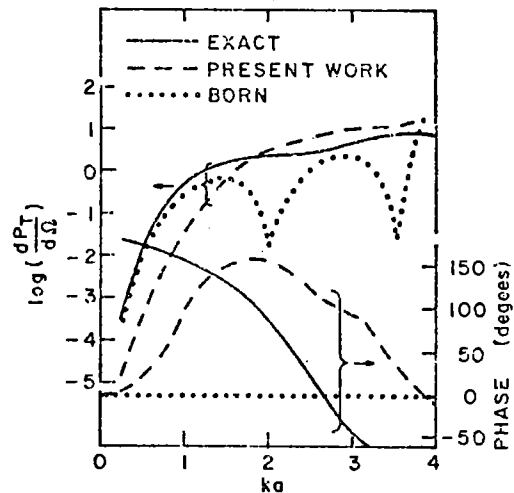


Fig. 5 Spherical cavity in Ti: Mode converted shear wave scattered at $\theta = 90^\circ$, power and phase versus ka for a ratio of radii of $4/3$.

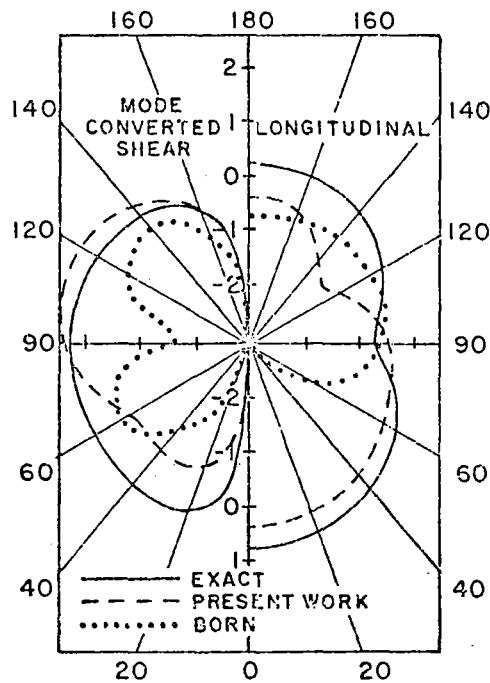


Fig. 6 Spherical cavity in Ti: Longitudinal and mode converted shear waves, log (power) versus θ for $ka = 2$ and ratio of radii of 4/3.

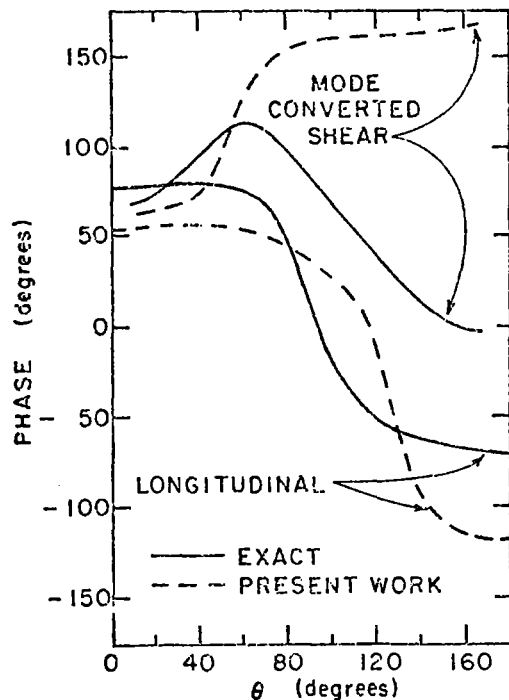


Fig. 7 Spherical cavity in Ti: Longitudinal and mode converted shear waves, phase versus θ for $ka = 2$ and ratio of radii of 4/3.

3. Non-ellipsoidal defects - To demonstrate the applicability of our method for non ellipsoidal defects, we considered backscattering by an Al inclusion in Ti, of the shape shown in Fig. 8. Three directions of incidence (of longitudinal waves) were studied, as also indicated on Fig. 8. The results for scattered longitudinal and shear power and phase are shown in comparison with that of a perfect sphere in Figs. 9-10. (No shear shown for sphere for backscattered.)

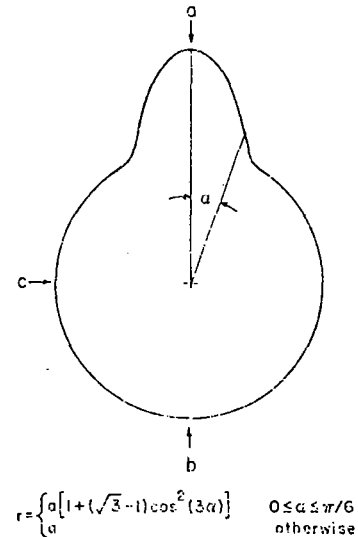


Fig. 8 Non-ellipsoidal defect: Three directions of incidence of the longitudinal wave. Defect is rotationally symmetric about the $\alpha = 0$ axis.

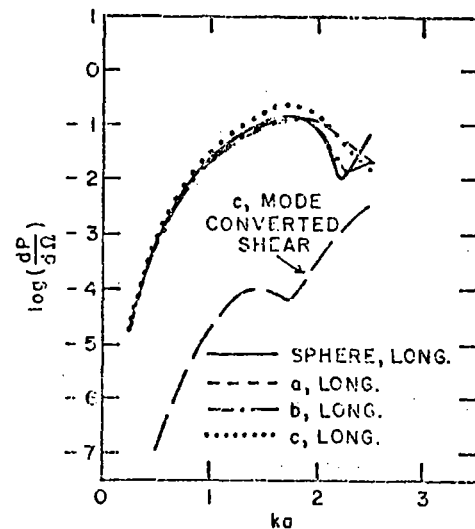


Fig. 9 Non-ellipsoidal defect, Al in Ti: Longitudinal and mode converted shear waves for three directions of incidence, log (power) versus ka .

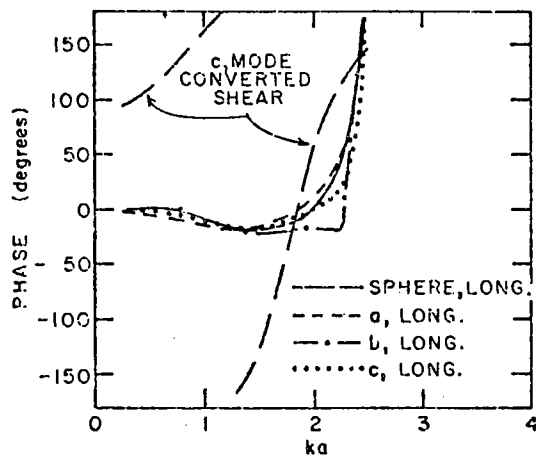


Fig. 10 Non-ellipsoidal defect, Al in Ti: Longitudinal and mode converted shear waves for three directions of incidence, phase versus ka .

SUMMARY AND DISCUSSION

We have developed an approximation method that can be used to study defects that are perturbations away from a spherical volume. We have found that this present theory constitutes a quite significant improvement over the Born Approximation. This is so in spite of the fact that we treat cases of large volume perturbations. The theory is not as good for the case of the cavity. This is reasonable because the other small parameters in the approximation (quantities like $\delta\rho/\rho$) are not small, but 1. This provides strong motivation to calculate the spherical Green's function and calculate with the DWBA. The DWBA is an expansion in both volume perturbations $\delta V/V$ and parameters like $\delta\rho/\rho$. To a given order in $\delta V/V$, all orders in $\delta\rho/\rho$ are included within DWBA. Thus reasonable results for cavities can be expected for small $\delta V/V$ for DWBA.

With this new approximation, investigation of non-ellipsoidal defects is now more feasible. Any shape that is a positive (larger volume) perturbation away from a sphere can be investigated. With the inclusion of the complete spherical Green's function into the calculation, negative perturbations from a sphere for inclusions will also be able to be handled. We intend to investigate a select class of interesting defects and continue in parallel with the development and inclusion of the spherical Green's function into the calculation. We hope to also learn about possible applications of phase information in classifying defects.

ACKNOWLEDGMENT

This research was sponsored by the Center for Advanced NDE, operated by the Science Center, Rockwell International, for the Defense Advanced Research Projects and the Air Force Materials Laboratory under Contract F33615-74-C-5180.

REFERENCES

1. J. E. Gubernatis, E. Domany, J. A. Krumhansl and M. Huberman, *J. Appl. Phys.* **48**, 2812(1977).
2. J. E. Gubernatis, to be published.
3. E. Domany, Interdisciplinary Program for Quantitative Flaw Definition, Special Report Third Year Effort, p. 70 (1977).
4. J. Richardson, these Proceedings.
5. B. Budiansky and J. R. Rice, preprint.
6. V. Varadan and V. Varadan, these proceedings.
7. A. Mucciandi, these proceedings and references therein.
8. B. R. Tittman, R. K. Elsley, H. Nadler and E. R. Cohen, Special Report Third Year Effort p. 82 (1977); L. Adler, *ibid.* p. 122.
9. J. E. Gubernatis, E. Domany and J. A. Krumhansl, *J. Appl. Phys.* **48**, 2804(1977).
10. C. F. Ying and R. Truell, *J. Appl. Phys.* **27**, 1086(1956); G. Johnson and R. Truell, *J. Appl. Phys.* **36**, 3466(1965); N. G. Einspruch, E. J. Witterholt and R. Truell, *J. Appl. Phys.* **31**, 806(1960). See also Ref. 1, Appendix A,B.
11. We thank B. Yanoff for programming assistance.